RSC Advances

PAPER

View Article Online
View Journal | View Issue

Cite this: *RSC Adv.*, 2025, **15**, 10816

Measuring interactions between Pickering emulsion droplets coated with casein–chitosan complex using optical tweezers†

Qifei Ma, [a] Huaizhou Jin,*[b] Weihong Wang[a] and Shangzhong Jin*[a]

Emulsions stabilized by protein/polysaccharide complexes have attracted great interest. However, the emulsion properties and interactions between droplets at the microscale require further investigation. In this work, the interaction forces between two rice bran oil droplets stabilized by casein–chitosan complexes, with a diameter of 3 ± 0.1 μm (pH 5.54 and no-salt), were measured under different aqueous conditions (pH and ionic strength) using optical tweezers. The measured force curves exhibited consistency with the interfacial layer conformation and interfacial charge, as determined through fluorescence spectroscopy and zeta-potential analysis. Furthermore, atomic force microscopy (AFM) and optical microscopy were employed to characterize the morphology and structural evolution of the emulsions under varying environmental conditions. Our results provide a useful method for studying the interaction forces between Pickering emulsion droplets with pN force resolution and reveal the correlation between interfacial layer properties and physical stability, offering deep insights into the stabilization mechanism of Pickering emulsions.

Received 25th December 2024
Accepted 19th March 2025

DOI: 10.1039/d4ra08998g

rsc.li/rsc-advances

1 Introduction

Rice bran oil has attracted researchers in recent years because of its high concentrations of health-promoting compounds, including tocopherols, tocotrienols, and γ-oryzanol. However, it possesses a negative flavor that consumers cannot find acceptable.[1] Therefore, to utilize its beneficial ingredients, rice bran oil is prepared into oil–water (O/W) emulsions for use in food, cosmetics, and pharmaceutical products.

However, emulsions[2,3] are inherently unstable multiphase systems that separate back into oil and water phases over time due to various instability mechanisms. To improve emulsion stability, most synthetic emulsifiers are used, but they may cause acute poisoning symptoms in humans and environmental pollution. As safety concerns gain more attention, natural emulsifiers such as proteins and polysaccharides are increasingly used in the food industry. Proteins are widely used as emulsifiers because of their excellent surface activities and amphiphilicity. However, a major drawback is their low solubility at their isoelectric points (pI), leading to a limited pH range where they exhibit satisfactory emulsifying activity. Additionally, their poor resistance to environmental stress (pH, ionic strength) greatly limits their practical applications.[4,5] Unlike proteins, polysaccharides usually have strong hydrophilicity and weak surface activity, but they enhance continuous phase viscosity by forming extended networks, thereby acting as emulsion stabilizers.[6] Consequently, the development of protein/polysaccharide complexes as novel emulsifiers and stabilizers has become a key research focus.[7,8] In this study, we used casein–chitosan complexes as an emulsifier.

Casein[9–12] is the most commonly used protein emulsifier in the food industry because of its extremely flexible structure (random coil), which can be attributed to its low hydrophobicity and high net charge. Casein usually exhibits better surface activity and emulsifying properties. However, as with other proteins, casein loses its emulsifying ability at a pI of 4.6, resulting in flocculation. The national standard for some foods, like salad sauces, is a maximum pH of 4.3. To utilize casein as an emulsifier, new methods must be developed to stabilize emulsions at pH 4.3. Chitosan[13,14] is a natural, non-toxic, biodegradable cationic polysaccharide, ideal for stabilizing emulsions due to its amphiphilic polyelectrolyte nature, combining both electrosteric and viscosifying stabilization mechanisms.

The researchers used the deprotonation[15] of chitosan to facilitate its interaction with casein, forming a stable complex that effectively stabilized the emulsions. The pK_a of chitosan is 6.5, meaning that when the pH is below this value, its $-NH_2$ undergoes protonation to form $-NH_3^+$, resulting in a positively charged polymer. Casein is predominantly positively charged at pH 2–4.6. However, several negatively charged groups remained

[a]College of Optical and Electronic Technology, China Jiliang University, Hangzhou 310018, China. E-mail: jinsz@cjlu.edu.cn

[b]Key Laboratory of Quantum Precision Measurement, College of Physics, Zhejiang University of Technology, Hangzhou 310014, China. E-mail: 18367198456@163.com

† Electronic supplementary information (ESI) available. See DOI: https://doi.org/10.1039/d4ra08998g

in casein. Thus, casein–chitosan complexes can form under weak acidic conditions *via* electrostatic attraction. The $-NH_3^+$ groups in chitosan interact with the $-COO^-$ groups in casein. The zeta-potential evolution of casein–chitosan complexes at different pH levels was previously measured by Ding *et al.*[15] However, the extent of this interaction is influenced by several factors. For example, at pH values close to or above the pK_a of chitosan, the protonation of amino groups decreases, reducing the positive charge density and weakening the interaction with casein. The pK_a of chitosan (~6.5) determines its protonation state and charge density, which in turn governs its ability to interact with casein through electrostatic interactions. In recent years, complexes of casein and chitosan have emerged, making full use of the adsorbed crosslinking layer to enhance the O/W emulsion stability.[15,16]

Currently, optical tweezers,[17,18] as a novel single-molecule level tool, allow for the manipulation and force measurement of dielectric particles without mechanical contact, offering nanometer and sub-millisecond spatial and temporal resolution, even pN force resolution. This makes them the method of choice for studying emulsion droplets with diameters below 10 μm. Since 2014, Julie *et al.*[19] qualitative measurements of the interactions between the emulsion droplets for the first time. Although they did not quantitatively analyze the force curve, the results are promising and imply that optical tweezers can be a useful tool for researchers exploring emulsion droplet interactions and stability. Griffiths *et al.*[20] proposed a method for measuring local salt concentration using optical tweezers. The Debye length can be fitted from the force–separation curves, and then the local salt concentration can be obtained using the relevant diffusion equation. In recent years, Chen *et al.* published numerous studies focusing on the measurement and analysis of the interactions between micron-sized droplets. They measured and analyzed the interaction forces between droplets stabilized by non-ionic surfactants,[21] ionic surfactants,[22,23] and polymers,[24] respectively. To date, emulsion stability has been studied based on the interface properties of single emulsifiers. However, in real life, emulsions are often stabilized by compound/mixed emulsifiers. The interfacial properties of compound/mixed emulsifiers that affect the stability of emulsions have not been investigated using optical tweezers, such as the interfacial properties of adsorbed layers and the conformation of emulsifiers under various environmental conditions (*e.g.*, pH and ionic strength).

In this study, we further investigated the properties of emulsions stabilized by casein–chitosan complexes to evaluate the effects of pH and ionic strength. In addition, we illustrate the stability mechanism based on the force behavior between two droplets at the microscale.

2 Method

2.1 Materials

Rice bran oil was purchased from a Hangzhou Yonghui Supermarket and used as the oil phase for all emulsions. Casein and chitosan were used as emulsifiers and stabilizers. Bovine serum albumin (BSA) was used to modify the surface of the sample chamber. All aqueous solutions were prepared using Milli-Q water with a resistance of 18.2 MΩ cm at 25 °C and acetic acid (CH_3COOH). Hydrochloric acid (HCl) and sodium hydroxide (NaOH) were used to adjust the pH value. All chemical agents were supplied by Aladdin.

The casein solution (2%, w/v) and chitosan solution (2%, w/v) were prepared by dissolving in deionized water and CH_3COOH solution, respectively, with magnetic stirring (1000 rpm) and ultrasonic treatment for 4 hours. The casein–chitosan complex solution was prepared by mixing 2% casein with 2% chitosan (volume ratio = 1 : 1) with stirring for 4 hours and then stored at 4 °C for later use. The preparation method and the casein to chitosan ratio were based on those reported by Yu *et al.*[8] They prepared stable Pickering emulsions with soybean protein and chitosan at a mass ratio of 1 : 1 and particle concentration of 2%.

Rice bran oil was added to the casein–chitosan complex (volume ratio = 1 : 1) and homogenized by a mechanical homogenizer (10 000 rpm) for 5 minutes, forming the original emulsion. The original emulsions should be diluted in solutions of different conditions (NaCl solution: 0 mM, 50 mM, 100 mM; $NaNO_3$ solution: 100 mM; KCl solution: 100 mM; pH: 2.25, 4.60, 5.54, 6.64, 7.10, 7.93, 8.20, 8.57) before measurements. All experiments were performed at 25 °C. Additionally, a 10^{-3} M Rhodamine 6G (R6G) solution was used to stain the emulsion droplets for confocal microscopy measurements.

2.2 Optical tweezers measurements

An m-trap™ optical tweezers instrument (Lumicks, Netherlands) was used to measure the interaction force between two Pickering emulsion droplets coated with casein–chitosan complexes in solutions with different pH and ionic strengths. The principle by which optical tweezers trap oil droplets is based on the change in photon momentum as the photon passes through an interface of two different refractive indices.[25,26] Optical tweezers enable precise control of the position and speed of droplets. The laser is a continuous wave infrared laser with a wavelength of 1064 nm and a maximum power of 10.0 W. The laser power was held constant at 2 W. A dual-laser optical tweezer is commonly used to study a couple of emulsion droplets. In a dual-laser configuration, one of the beads/droplets (held in a steerable trap) moves toward the other bead/droplet (held in a fixed trap). To exclude the effects of hydrodynamic forces, the approaching velocity is usually adjusted below 1.0 μm s^{-1}, and the forces between the two droplets can be calculated as they approach each other and begin to interact.

The prepared emulsions were then pumped into the sample chamber; a schematic of the flow is shown in Fig. 1(a). The chamber included three parts: a regular coverslip (thickness of 0.175 mm) as the bottom glass, a regular glass slide (thickness of 1 mm) as the top glass, and PMMA double-sided tape was used as a side wall to maintain a 100 μm height between the two glass pieces. To limit the adhesion between the droplets and chamber, the chamber was treated with 1 mg per mL BSA solution for 60 minutes before injection of the emulsion

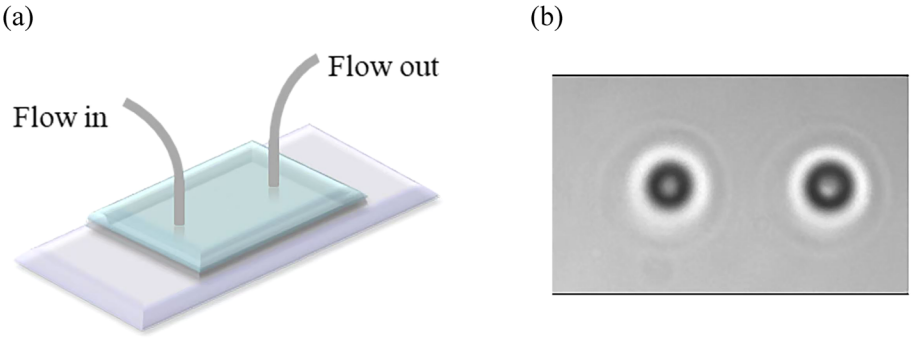

Fig. 1 (a) Schematic of the sample chamber. (b) A pair of droplets trapped using optical tweezers.

droplets. In our experiments, we adjusted the pH of the BSA solution to accommodate samples with different electric charges. Note that strongly alkaline BSA is viscous, which is undesirable for sample measurements. Therefore, for negatively charged samples, the BSA solution charge was regulated at approximately −12 mV. Two droplets were trapped in two traps, as shown in Fig. 1(b).

2.3 Zeta (ζ)-potential

The ζ-potentials of emulsion droplets in NaCl solutions of different concentrations and at different pH values were measured using a nanoparticle SZ-100V2 (Horiba, Japan). All measurements were performed at 25 °C.

2.4 Fluorescence spectroscopy

Fluorescence spectroscopy (Aqualog, Horiba, Japan) was employed to quantify the binding of chitosan and casein and the conformation changes in casein–chitosan complexes on droplet interactions by measuring the changes in fluorescence emission intensity and wavelength shifts of emulsions under different conditions. The sample (1 mL) was excited at 280 nm with a resolution of 2.2 nm. All measurements were performed at 25 °C.

2.5 Atomic force microscope

Three silicon substrates were exposed to O_2 plasma for 5 minutes at a power of 100 W. Then, 2% casein, 2% chitosan, and their complexes were dropped on the three silicon substrates, respectively, until they were dried at room temperature.

Images of casein, chitosan and complexes were collected using an Atomic Force Microscope (AFM, Bruker Innova) operated in tapping mode. Ultrasharp, non-contact silicon cantilevers with a nominal tip radius of <10 nm were driven at oscillation frequencies in the range of 20–26 kHz.

2.6 Optical microscope

An optical microscope (Olympus BX53, Japan) and a confocal microscope (Nikon C2, Japan) were used to observe the aggregation behavior of the emulsion droplets under various aqueous conditions.

3 Results and discussion

3.1 Characterization of casein–chitosan complexes

The microphotographs of casein, chitosan, and their complexes were obtained by AFM, as shown in Fig. 2(a)–(c). Casein appeared as heterogeneous ellipsoids with particle heights between 30 and 70 nm, whereas chitosan appeared as flat blocks with particle heights between 60 and 80 nm, as shown in Fig. 2(d)–(f). The surface of the casein–chitosan complex is rough, and its particle size reaches 20 nm, indicating a high level of structural interaction within the complex, which contributes to its good stability. Yu *et al.*[8] also used SEM to study soybean protein isolate/chitosan hydrochloride complexes and obtained similar results. Additionally, Milenkova *et al.* verified that the sizes of the casein–chitosan complexes were similar to the results obtained using the DLS technique. The complex size affects the interfacial layer thickness. Cai *et al.*[2] concluded that the interfacial layer thickness of casein-stabilized emulsions is approximately 13–15 nm, which is consistent with the size of our complexes.

To demonstrate the binding balance between casein and chitosan and to observe the structural transition that may occur during the binding of chitosan to protein, intrinsic fluorescence can be used. Tryptophan is a strong intrinsic fluorophore, highly sensitive to the polarity of its environment in proteins.[27] The characteristics of the fluorescence emission spectrum of tryptophan depend on the environment.

The maximum emission wavelength is about 350 nm when tryptophan is fully exposed to a polar aqueous environment, whereas in a very hydrophobic environment, it can be as low as 310 nm.[28] In addition to the position of the maximum emission, the local environment modulates the intensity of the fluorescence emission. In general, the quantum yield is higher in an apolar environment, such as the core of folded proteins, than in a polar environment. These properties can be used to monitor structural alterations in proteins. Since the excited state of the indole ring can donate electrons to neighboring molecules, the addition of chitosan can quench the maximum fluorescence intensity.[28] Yazdi *et al.* quantified the binding between curcumin and casein using tryptophan quenching fluorescence spectroscopy.[29] The typical fluorescence emission spectrum of casein in the presence and absence of chitosan at 280 nm

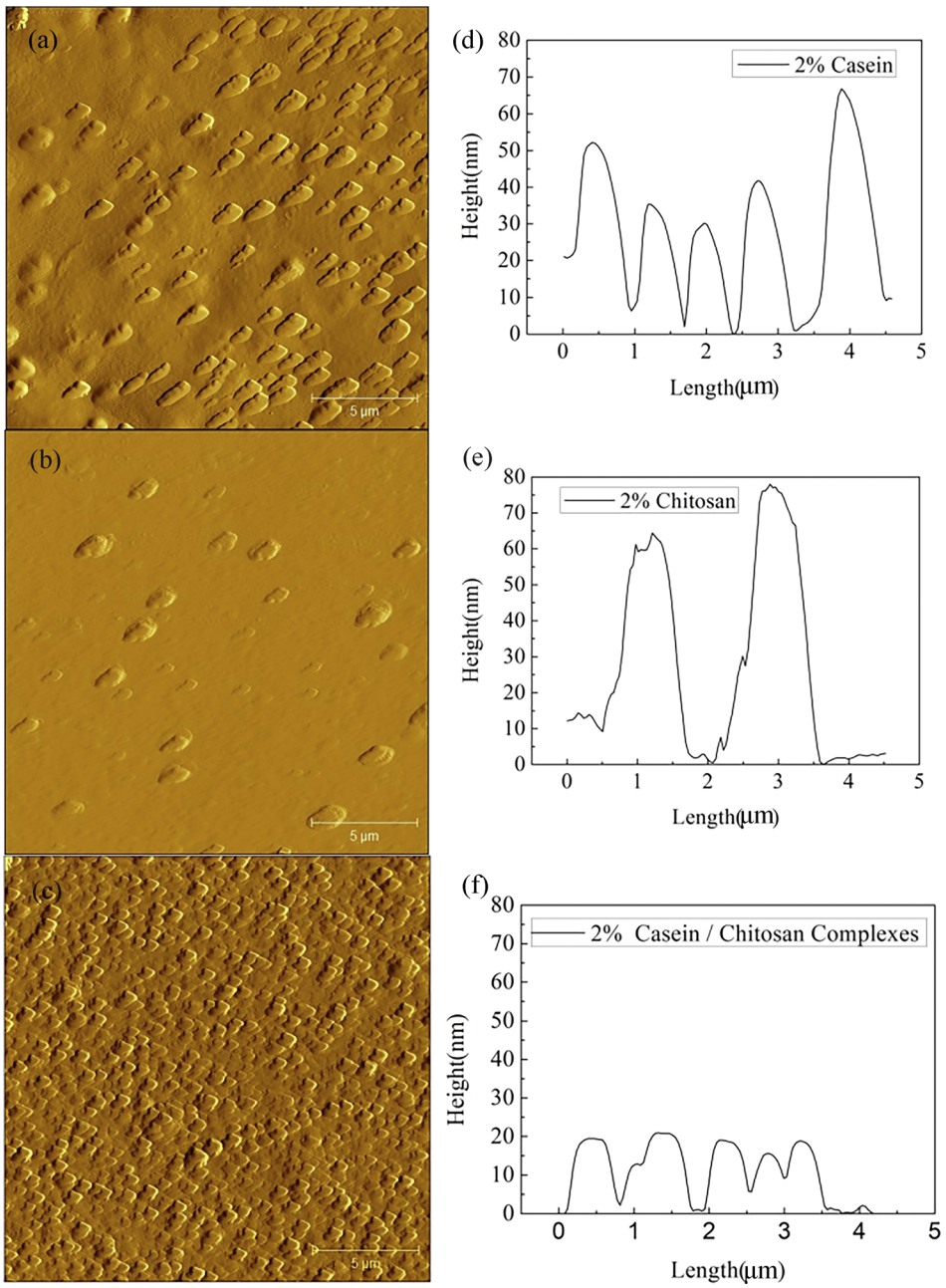

Fig. 2 (a–c) Microphotographs of 2% casein, 2% chitosan and 2% casein–chitosan complexes and (d–f) heights of 2% casein, 2% chitosan and 2% casein–chitosan complex.

excitation is shown in Fig. 3. The maximum emission wavelength shifted blue by approximately 5 nm, indicating a shift to a more hydrophobic environment where more chitosan bound to casein, resulting in casein unfolding. It is well-known that enhanced protein surface hydrophobicity makes the hydrophilic part of the molecule more easily oriented to the water phase, and the non-polar groups more easily oriented to the oil phase, causing the interfacial tension to drop faster.[30] The addition of chitosan not only makes casein more hydrophobic but also changes its conformation. The effect of the compound emulsifier was better than that of casein alone. When the casein–chitosan complex is adsorbed on the droplet surface, the maximum emission wavelength changes from 317.5 to 309.6 nm, indicating a shift to a more hydrophobic environment, as shown in Fig. 3. Thus, once the casein–chitosan complexes are adsorbed on the O/W surface, they rearrange at the interface.[31]

3.2 Characterization of Pickering emulsions

3.2.1 Effects of salt concentration. In this study, we first selected three pairs of droplets with a diameter of 3 ± 0.1 μm to verify data repeatability, as shown in Fig. 4(a). When two droplets approached each other, the repulsive force was approximately 30 pN, indicating that the emulsion had

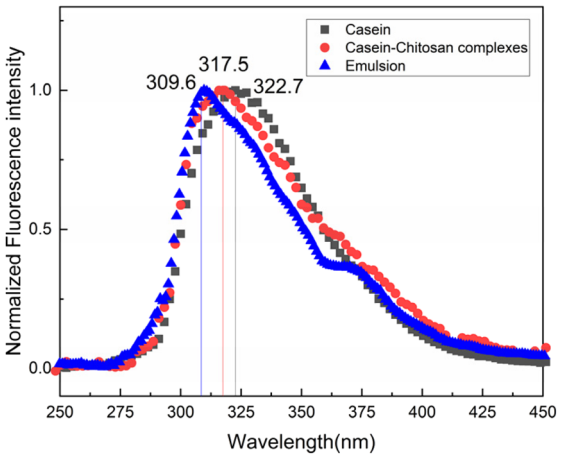

Fig. 3 Fluorescence spectrum of casein, casein–chitosan complexes and emulsion stabilized by casein–chitosan complexes. All samples were uniformly diluted in deionized water at identical dilution ratios.

relatively good homogeneity and that the instrument was stable. We also measured the force curves of the emulsions based on different oil phases under the same conditions ($C_{NaCl} = 0$ mM, pH = 5.57) (in the ESI Fig. S1†).

Then, experimental conditions with three different salt concentrations were designed to study the effect of the salt concentration on the interaction force and stability of the emulsion. The pH values of the three samples were maintained at 5.5.

The interaction forces between two droplets with a diameter of 3 ± 0.1 μm were measured using optical tweezers for different salt concentrations at an approaching velocity of less than 1 μm s^{-1}. Repulsive interaction forces were observed in the force curves, as shown in Fig. 4(b). Under the same force load, two droplets require a longer interaction scale[21,22] in a 100 mM NaCl solution than in an unsalted solution. Within the DLVO framework,[32] the total interaction force between particles is the sum of the electrostatic repulsion and van der Waals attraction. At small separations, electrostatic repulsion typically occurs. However, as the distance between particles decreases further, van der Waals attraction may become predominant, leading to droplet aggregation. To maintain emulsion stability at high salt concentrations, strategies such as modifying the solution conditions to increase the interparticle distance are required. We also conducted force measurement experiments using $NaNO_3$ and KCl at the same concentration (in the ESI Fig. S2†).

We also supplemented the collision experiment, as illustrated in ESI Fig. S4.† According to some arrested coalescence,[33–35] which is usually observed in Pickering emulsions, we discuss the stability of this Pickering emulsion in the ESI.†

The DLVO theory[32] has been widely applied to describe the stability of colloidal spheres in aqueous solution, which includes both VDW and EDL interactions, as shown in eqn (1)

$$F = F_{VDW}(h) + F_{EDL}(h) = -\frac{A_H R}{6h^2} + \left(\frac{e^2 Z^2}{8\pi\varepsilon_0\varepsilon_r R^3}\right)\kappa^{-1}\exp(-\kappa h) \quad (1)$$

where A_H is the Hamaker constant between two spheres (with radius R) in an aqueous solution, and h is the surface-to-surface distance between two spheres, Z is a process variable, R is the radius of the spheres, ε_0 is the permittivity of vacuum, ε_r is the relative permittivity of the aqueous phase solution, e is the elementary charge, κ^{-1} is the Debye length.

According to DLVO theory, the destruction of the electrostatic double-layer increases gradually with increasing salt concentration. We can use eqn (2)[36] to calculate the Debye length.

$$\kappa^{-1} = \sqrt{\frac{\varepsilon_0\varepsilon_r k_B T}{2\times 10^3 N_A e^2 I}} \quad (2)$$

where k_B is the Boltzmann constant, T is the thermodynamic temperature, and I is the intensity of the ions in aqueous solution. I can be calculated using eqn (3).[36]

$$I = \frac{1}{2}\sum_i c_i z_i^2 \quad (3)$$

where c_i is the ion concentration, z_i is the electric charge of the ions. It can be explained that an increase in salt reduces Debye length, leading to shorter-ranged repulsion and typically resulting in emulsion destabilization.

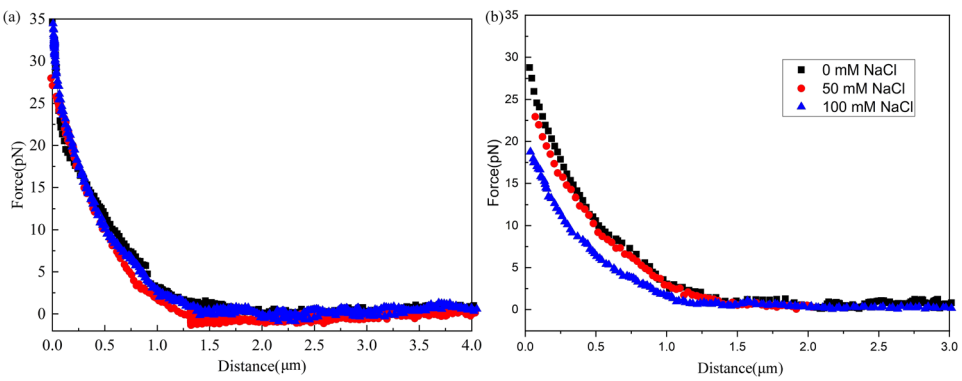

Fig. 4 (a) Force–distance curves of three pairs of droplets with a diameter of 3 ± 0.1 μm (pH = 5.54, no-salt). (b) Force–distance curve at different salt concentration solutions.

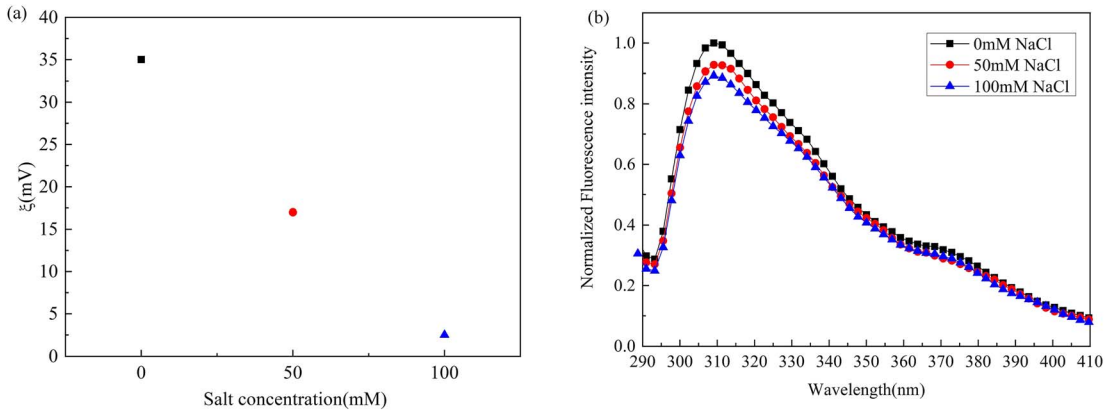

Fig. 5 (a) Zeta potentials of emulsions at different salt concentration solutions. (b) Fluorescence spectrum of emulsions diluted in solutions with varying salt concentrations at an identical dilution ratio.

The zeta potentials of the emulsions were also measured at various NaCl concentrations. A higher salt concentration would have a negative influence on the absolute zeta potential, as shown in Fig. 5(a). It is easy to explain the decrease in the absolute value of zeta potential with increasing salt concentration by using eqn (4).[22]

$$\zeta = 0.0514 \sinh^{-1}\left[\frac{8.24 \times 10^5 \Gamma_R}{\sqrt{C_{NaCl}}}\right] \quad (4)$$

where ζ is the absolute value of the zeta potential between droplets, Γ_R is the adsorption amount of molecules, and C_{NaCl} is the salt concentration.

To understand the conformation changes of casein–chitosan complexes after salt addition, we measured the fluorescence spectra of the emulsions, as shown in Fig. 5(b). The emission intensity decreased as the NaCl concentration increased from 0 to 100 mM. The salt may disrupt the electrostatic interaction between casein and chitosan by shielding the charged active sites on the two biopolymers, thus requiring more chitosan to enclose the casein, which promotes bridge flocculation.

Optical microscope observations confirmed that the droplet characteristics changed with salt concentration. The increase in salt concentration led to aggregation of the emulsion, consistent with the interaction results between the droplets, as shown in Fig. 6.

3.2.2 Effects of pH. We designed several experimental conditions for different pH solutions to study the effect of pH on the interaction forces and emulsion stability.

In the acidic region, as the pH decreases, two droplets require a longer interaction scale, as shown in Fig. 7. At casein's pI, emulsions remain more stable than at pH 2.55. At pH 4.6, the zeta potential is 57.5 mV, not 0 mV. This result can be attributed to the chitosan wrapped around the casein, which provided steric repulsion and stabilization for the casein micelles. At pH 4.6 (near the pI), the electrostatic attraction between casein and chitosan decreases because casein carries

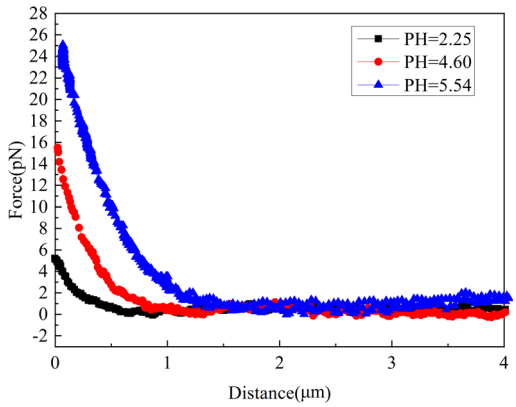

Fig. 7 Force–distance curve in the acidic solutions.

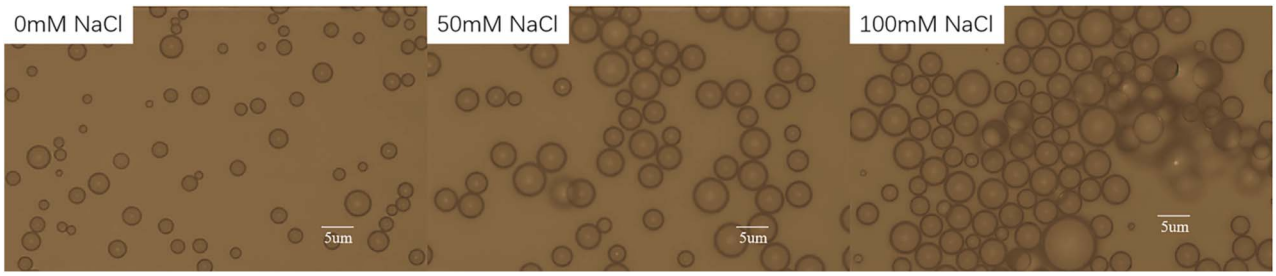

Fig. 6 Optical microscopy images of O/W emulsions stabilized by 2% casein–chitosan complex at different salt concentrations.

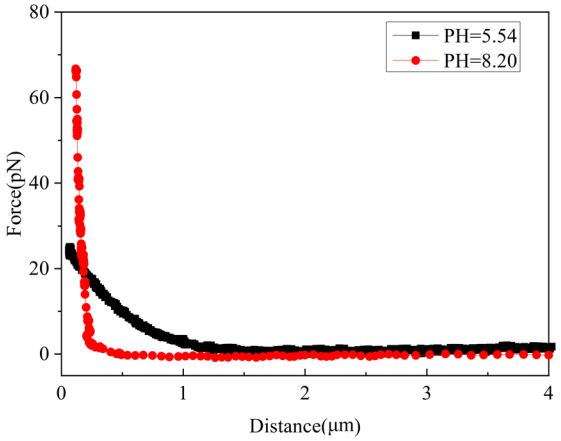

Fig. 8 The slope of the force–distance curve in the acidic/alkaline solutions.

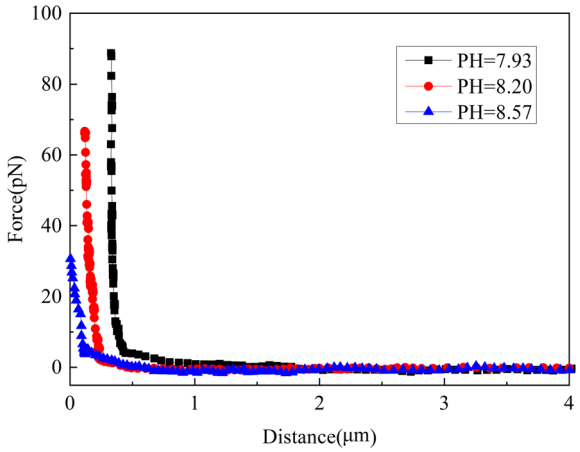

Fig. 9 Force–distance curve in the alkaline solutions.

almost a net zero charge. Therefore, the stability and binding site of the complex are reduced, and the binding of casein to chitosan is looser. At pH 5.5, the repulsive force occurs at a much longer distance, which is not consistent with the zeta potential. However, many authors have discussed this special position between pH 5 and 5.5. Dan *et al.* noted that the interfacial layer of β-casein-stabilized water/hexane emulsions reached the maximum dynamic elasticity value and the most compact conformation at pH 5.[37] Ding *et al.* measured the size and light scattering intensity of casein–chitosan complexes and verified that at pH 5.5, the strongest electrostatic interaction occurs between casein and chitosan, leading to the most compact complexation.[15]

The electrostatic interaction remained at the same level at pH 8.20 and pH 5.54 because the absolute values of the zeta potential at these pH levels were almost the same. However, due to the differing charge properties of casein and chitosan, their binding mechanisms varied. At pH 8.2, some chitosan can easily obtain deprotonated amines because of the free amino groups in the chitosan molecules. Thus, chitosan with free protonated amino groups may bind to negatively charged patches on the surface of casein. When the pH is increased to the alkaline region, there is a significant difference in the slope of force–distance curves as the droplets come into contact, as shown in Fig. 8. The droplets in the acidic solution exhibit higher deformability. Julie *et al.*[19] compared the slopes of the FD curves between polystyrene beads and emulsion droplets.

At pH values between 6.64 and 7.1, which are close to the pK_a of chitosan, a net zero charge is present on the partial chitosan surface, resulting in a zeta potential of zero. As the pH increases in the alkaline region, although the absolute value of zeta-potential increases, the repulsive force still occurs at shorter surface distances, and emulsions gradually lose their stability, as shown in Fig. 9. The zeta-potential measurement of the mixture reflects the total charge, including the contributions of both casein and chitosan. While casein and chitosan contribute to zeta-potential measurements, they show a higher attraction in force measurements. Additionally, under a confocal microscope, many micelles were observed in the alkaline solution (in the ESI Fig. S3†). According to Chakraborty's analysis of pH-induced structural transitions of caseins, in strongly alkaline conditions, caseins might unfold and release some bound

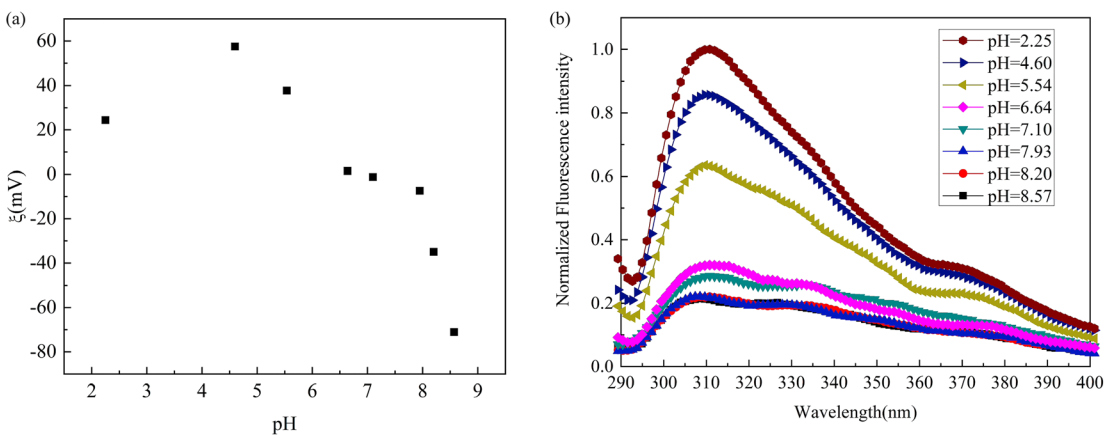

Fig. 10 (a) Zeta potentials of emulsions in solutions with different pH values; (b) fluorescence spectrum of the emulsions diluted in solutions with different pH levels at identical dilution ratios.

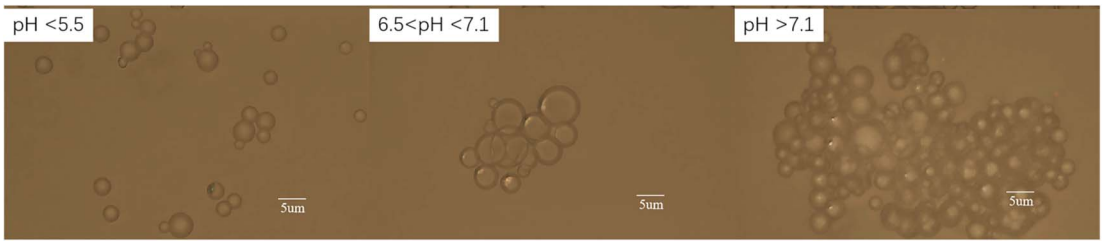

Fig. 11 Optical microscopy images of O/W emulsions stabilized by 2% casein–chitosan complex under different pH solutions.

chitosan into the bulk solvent. This can explain the FD curve and zeta potential in alkaline solutions.[12]

Fig. 10(a) shows the zeta potentials in different pH solutions. Ding *et al.*[15] hypothesized that highly hydrophilic chitosan packs some individual casein lamellas together and adheres tightly to their surface, forming a core–shell structure. The addition of chitosan mitigated the protein drawbacks and improved the stability of the emulsions.

Altering the pH of a solution may cause caseins at the O/W interface to adopt different conformations, leading to variable interfacial properties and affecting emulsion stability.[38] To analyze the effect of conformation changes in casein–chitosan complexes on droplet interactions, fluorescence spectra of the emulsions in different pH environments were measured, as shown in Fig. 10(b). As the pH increases to 6.64, the caseins gradually unfold. In the alkaline region, the conformation changes minimally, indicating that casein is almost fully unfolded. The fluorescence spectrum confirms this behavior. In the acidic region, steric forces are dominant. In the alkaline region, depletion forces begin to occur, affecting the stability of the emulsions. Emulsions stabilized by casein–chitosan complexes exhibit better stability in acidic conditions.

Optical microscope observations confirmed that the droplet characteristics changed with the pH of the solutions. The stability was better in acid, and the coalescence or associative phase separation between casein and chitosan can occur under pH $\geq$ pK_a, leading to emulsion instability, as shown in Fig. 11. This result is consistent with the results of the interactions between the droplets.

4 Conclusion

In this work, we measured the interaction force between two rice bran oil droplets stabilized by casein–chitosan complexes with a diameter of 3 μm under different aqueous conditions using optical tweezers, which verified the results obtained from bulk sample instruments.

Firstly, we discuss the influence of salt on the Pickering emulsion. The addition of salt promoted flocculation and sedimentation and reduced emulsion stability. Salt not only shielded the charge on the surface of the emulsions but also disrupted the electrostatic interactions between proteins and polysaccharides.

Secondly, we explored the influence of pH on the emulsion stability. The addition of chitosan significantly improved casein stability at pH 4.6, broadening the casein pH range. This study demonstrated the applications of rice bran oil and protein–chitosan complexes as emulsifiers in acidic and low salt concentrations, which not only avoids the unpleasant flavor of rice bran oil but also stabilizes it.

Optical tweezers offer a unique advantage in the study of Pickering emulsions, enabling the exploration of emulsion stabilization mechanisms at the microscopic level as well as the response of emulsions to external stimuli. These studies not only enhanced our fundamental understanding of Pickering emulsions but also provided new avenues for their application in drug delivery and therapy. For instance, emulsion droplets can serve as microreactors for various biochemical reactions. However, current systems primarily focus on improving catalytic efficiency and often overlook critical challenges such as slow reaction kinetics at the oil–water interface, the lack of precise control over the entire reaction process, and limited chemical communication between droplets.

Integrating optical tweezers into this research paradigm has transformative potential. Optical tweezers not only enable precise manipulation of individual droplets but also facilitate *in situ* investigations into the effects of external stimuli on emulsion behavior. For example, by coupling optical tweezers with additional light sources, instantaneous demulsification or droplet fusion can be achieved, allowing dynamic control of the reaction environment. Moreover, when combined with advanced analytical techniques such as Raman spectroscopy and fluorescence imaging, optical tweezers enable real-time monitoring and analysis of content exchange during biochemical reactions. This multimodal approach provides unprecedented insights into reaction dynamics and interfacial phenomena, paving the way for the design of more efficient and controllable microreactor systems.

Data availability

The authors confirm that the data supporting the findings of this study are available within the article.

Author contributions

Qifei Ma: conceptualization of this study, methodology, software, investigation, original draft preparation, writing – review and editing. Weihong Wang: methodology. Huaizhou Jin: resource, review and editing and funding acquisition.

Shangzhong Jin: writing review and editing, funding acquisition and supervision.

Conflicts of interest

No potential conflict of interest was reported by the author(s).

Acknowledgements

We are grateful for the continued financial support from the National Natural Science Foundation of China (No. 22202167), the National Key Research and Development Project of China (No. 2023YFF0613603), and the Provincial Science and Technology Plan Project: Micro and Nano Preparation and Photoelectronic Detection (No. 03014/226063).

References

1 P. Sneh, K. Manoj, K. S. Anil and S. P. Sukhvinder, *Rice Sci.*, 2021, **28**, 217.
2 Z. Cai, Y. Wei, A. Shi, J. Zhong, P. Rao, Q. Wang and H. Zhang, *Adv. Colloid Interface Sci.*, 2023, **313**, 102863.
3 Y. Deng, M. Dai, Y. Wu and C. Peng, *Crit. Rev. Environ. Sci. Technol.*, 2023, **53**, 1254.
4 J. Zheng, P. V. der Meeren and W. Sun, *Aggregate*, 2024, **5**, e449.
5 R. S. H. Lam and M. T. Nickerson, *Food Chem.*, 2013, **141**, 975.
6 Y. Cai, X. Deng, T. Liu, M. Zhao, Q. Zhao and S. Chen, *Food Hydrocolloids*, 2018, **79**, 391.
7 L. Lv, C. Fu, F. Zhang and S. Wang, *Food Chem.*, 2019, **275**, 273.
8 S.-J. Yu, S.-M. Hu, Y.-Z. Zhu, S. Zhou, S. Dong and T. Zhou, *Int. J. Biol. Macromol.*, 2023, **250**, 126146.
9 P. J. García-Moreno, A. Frisenfeldt Horn and C. Jacobsen, *J. Agric. Food Chem.*, 2014, **62**, 1142.
10 P. Wang, C. Chen, H. Guo, H. Zhang, Z. Yang and F. Ren, *Food Hydrocolloids*, 2018, **77**, 689.
11 Wusigale, L. Liang and Y. Luo, *Trends Food Sci. Technol.*, 2020, **97**, 391.
12 A. Chakraborty and S. Basak, *J. Photochem. Photobiol., B*, 2007, **87**, 191.
13 Y. Liu, Y. Fan, X. Wu, Y. Lu and J. Yi, *Food Funct.*, 2020, **11**, 1740.
14 C. Yan, D. J. McClements, Y. Zhu, L. Zou, W. Zhou and W. Liu, *J. Agric. Food Chem.*, 2019, **67**, 10937.
15 L. Ding, Y. Huang, X. Cai and S. Wang, *Carbohydr. Polym.*, 2019, **208**, 133.
16 F. Zhang, X. Cai, L. Ding and S. Wang, *Food Hydrocolloids*, 2021, **111**, 106211.
17 K. C. Neuman and A. Nagy, *Nat. Methods*, 2008, **5**, 491.
18 H. Zhang and K.-K. Liu, *J. R. Soc. Interface*, 2008, **5**, 671.
19 J. Nilsen-Nygaard, M. Sletmoen and K. I. Draget, *RSC Adv.*, 2014, **4**, 52220.
20 M. R. Griffiths, A. Raudsepp, K. M. McGrath and M. A. K. Williams, *RSC Adv.*, 2016, **6**, 14538.
21 A. Chen, S.-W. Li, D. Jing and J.-H. Xu, *Chem. Eng. Sci.*, 2019, **193**, 276.
22 A. Chen, S.-W. Li, F.-N. Sang, H.-B. Zeng and J.-H. Xu, *J. Colloid Interface Sci.*, 2018, **532**, 128.
23 A. Chen, Y. Jing, F.-N. Sang, S.-W. Li and J.-H. Xu, *Chem. Eng. Sci.*, 2018, **181**, 341.
24 A. Chen, S. Li and J. Xu, *Chin. J. Chem. Eng.*, 2020, **28**, 1368.
25 A. Ashkin, J. M. Dziedzic, J. E. Bjorkholm and S. Chu, *Opt. Lett.*, 1986, **11**, 288.
26 A. Ashkin, *Phys. Rev. Lett.*, 1970, **24**, 156.
27 M. R. Eftink, *Methods Biochem. Anal.*, 1991, **35**, 127.
28 *Principles of Fluorescence Spectroscopy*, ed. J. R. Lakowicz, Springer US, Boston, MA, 2006.
29 S. Rahimi Yazdi and M. Corredig, *Food Chem.*, 2012, **132**, 1143.
30 R. Li, X. Wang, J. Liu, Q. Cui, X. Wang, S. Chen and L. Jiang, *J. Agric. Food Chem.*, 2019, **67**, 4089.
31 C.-H. Tang, *Crit. Rev. Food Sci. Nutr.*, 2017, **57**, 2636.
32 V. Agmo Hernández, *ChemTexts*, 2023, **9**, 10.
33 H. Kumar, S. Upendar, E. Mani and M. G. Basavaraj, *J. Colloid Interface Sci.*, 2023, **633**, 166.
34 A. B. Pawar, M. Caggioni, R. Ergun, R. W. Hartel and P. T. Spicer, *Soft Matter*, 2011, **7**, 7710.
35 B. T. Lobel, D. Baiocco, M. Al-Sharabi, A. F. Routh, Z. Zhang and O. J. Cayre, *Langmuir*, 2025, **41**, 550.
36 O. Aarøen, E. Riccardi and M. Sletmoen, *RSC Adv.*, 2021, **11**, 8730.
37 A. Dan, R. Wüstneck, J. Krägel, E. V. Aksenenko, V. B. Fainerman and R. Miller, *Food Hydrocolloids*, 2014, **34**, 193.
38 R. Wüstneck, V. B. Fainerman, E. V. Aksenenko, Cs. Kotsmar, V. Pradines, J. Krägel and R. Miller, *Colloids Surf., A*, 2012, **404**, 17.